


Accelerating discovery, enabling scientists
 Discover the benefits of using spectral flow cytometry for high-parameter, high-throughput cell analysis



SONY
 Download Tech Note



Id2 Collaborates with Id3 To Suppress Invariant NKT and Innate-like Tumors

This information is current as of August 9, 2022.

Jia Li, Sumedha Roy, Young-Mi Kim, Shibo Li, Baojun Zhang, Cassandra Love, Anupama Reddy, Deepthi Rajagopalan, Sandeep Dave, Anna Mae Diehl and Yuan Zhuang

J Immunol 2017; 198:3136-3148; Prepublished online 3 March 2017;

doi: 10.4049/jimmunol.1601935

<http://www.jimmunol.org/content/198/8/3136>

Supplementary Material <http://www.jimmunol.org/content/suppl/2017/03/03/jimmunol.1601935.DCSupplemental>

References This article **cites 95 articles**, 33 of which you can access for free at: <http://www.jimmunol.org/content/198/8/3136.full#ref-list-1>

Why *The JI*? Submit online.

- **Rapid Reviews! 30 days*** from submission to initial decision
- **No Triage!** Every submission reviewed by practicing scientists
- **Fast Publication!** 4 weeks from acceptance to publication

**average*

Subscription Information about subscribing to *The Journal of Immunology* is online at: <http://jimmunol.org/subscription>

Permissions Submit copyright permission requests at: <http://www.aai.org/About/Publications/JI/copyright.html>

Email Alerts Receive free email-alerts when new articles cite this article. Sign up at: <http://jimmunol.org/alerts>



Id2 Collaborates with Id3 To Suppress Invariant NKT and Innate-like Tumors

Jia Li,^{*1} Sumedha Roy,^{*1} Young-Mi Kim,[†] Shibo Li,[†] Baojun Zhang,^{*} Cassandra Love,[‡] Anupama Reddy,[‡] Deepthi Rajagopalan,[‡] Sandeep Dave,[‡] Anna Mae Diehl,[§] and Yuan Zhuang^{*}

Inhibitor of DNA binding (Id) proteins, including Id1–4, are transcriptional regulators involved in promoting cell proliferation and survival in various cell types. Although upregulation of Id proteins is associated with a broad spectrum of tumors, recent studies have identified that Id3 plays a tumor-suppressor role in the development of Burkitt's lymphoma in humans and hepatosplenic T cell lymphomas in mice. In this article, we report rapid lymphoma development in *Id2/Id3* double-knockout mice that is caused by unchecked expansion of invariant NKT (iNKT) cells or a unique subset of innate-like CD1d-independent T cells. These populations began to expand in neonatal mice and, upon malignant transformation, resulted in mortality between 3 and 11 mo of age. The malignant cells also gave rise to lymphomas upon transfer to *Rag*-deficient and wild-type hosts, reaffirming their inherent tumorigenic potential. Microarray analysis revealed a significantly modified program in these neonatal iNKT cells that ultimately led to their malignant transformation. The lymphoma cells demonstrated chromosome instability along with upregulation of several signaling pathways, including the cytokine–cytokine receptor interaction pathway, which can promote their expansion and migration. Dysregulation of genes with reported driver mutations and the NF- κ B pathway were found to be shared between *Id2/Id3* double-knockout lymphomas and human NKT tumors. Our work identifies a distinct premalignant state and multiple tumorigenic pathways caused by loss of function of Id2 and Id3. Thus, conditional deletion of *Id2* and *Id3* in developing T cells establishes a unique animal model for iNKT and relevant innate-like lymphomas. *The Journal of Immunology*, 2017, 198: 3136–3148.

A significant portion of cancer research is dedicated to the identification of underlying factors that contribute to the hallmarks of tumorigenesis (1–3), such as dysregulated proliferation and self-renewal (4, 5). All four members of the inhibitor of DNA binding (Id) family (Id1–4) of helix–loop–helix transcription factors share the ability to promote proliferation and a stem cell–like dedifferentiated state (6, 7) and are often upregulated in various cancer types (8–12). Id protein activity is also found to be directly correlated with tumor initiation, progression,

and sensitivity to therapy (7). Therefore, they are deemed as attractive tumor therapeutic targets based on the use of small molecule inhibitors and Id-binding peptides in mouse models and cancer cell lines (10, 13–16). In contrast, deep sequencing of human Burkitt's lymphoma samples has revealed loss-of-function mutations in *Id3* in a large subset of patients, supporting the tumor-suppressor role of Id3 in some contexts (17–19). *Id3*^{-/-} mice have also been reported to develop $\gamma\delta$ hepatosplenic T cell lymphoma as a consequence of $V\gamma 1.1^+V\delta 6.3^+$ $\gamma\delta$ T cell population expansion (20). Although there are some reports suggesting a context-dependent role for Id4 in tumor progression or suppression (21–23), there is only limited evidence in favor of a tumor-suppressive role for Id2 (24).

Id proteins are primarily considered inhibitors of E proteins, the founding members of basic helix–loop–helix transcription factors (25). Id2 and Id3, which are highly expressed in lymphocytes, are known for their critical roles in suppressing E protein activity at various stages to allow conventional $\alpha\beta$ T cell development (26, 27). They have also been recently described to repress innate-like $\gamma\delta$ and invariant NKT (iNKT) cell development (28–37).

Innate-like T cells are unique populations of T cells that derive their name from an innate cell–like ability to quickly secrete a myriad of cytokines in response to Ag (38, 39). These populations play key roles in providing protection against tumors and certain infectious and autoimmune diseases, even though they are usually present in negligible proportions compared with conventional T cells (40, 41). The best characterized innate-like T cells are $V\gamma 1.1V\delta 6.3$ $\gamma\delta$ T cells and iNKT cells, but other cell types, like mucosal-associated invariant T cells, are also included in this category (42). iNKT cells express a semi-invariant TCR, $V\alpha 14J\alpha 18$, which allows them to be identified by α -GalCer–loaded CD1d tetramers (CD1dTets) (43).

^{*}Department of Immunology, Duke University Medical Center, Durham, NC 27710; [†]Department of Pediatrics, Oklahoma University Health Sciences Center, Oklahoma City, OK 73014; [‡]Duke Institute for Genome Sciences and Policy, Duke University, Durham, NC 27710; and [§]Department of Medicine, Duke University Medical Center, Durham, NC 27710

¹J.L. and S.R. contributed equally to this work.

ORCID: 0000-0003-3070-8635 (J.L.); 0000-0002-2766-0071 (Y.-M.K.); 0000-0002-7786-4304 (B.Z.).

Received for publication November 14, 2016. Accepted for publication February 7, 2017.

This work was supported by National Institutes of Health Grants R01 GM059638 and P01 AI102853 (to Y.Z.).

The microarray data presented in this article have been submitted to the Gene Expression Omnibus repository (<https://www.ncbi.nlm.nih.gov/projects/geo>) under accession number GSE83761.

Address correspondence and reprint requests to Prof. Yuan Zhuang, Jones Building, Room 326, 207 Research Drive, Duke University, Durham, NC 27710. E-mail address: yzhuang@duke.edu

The online version of this article contains supplemental material.

Abbreviations used in this article: CD1dTet, CD1d tetramer; DN, double-negative; DP, double-positive; Id, inhibitor of DNA binding; iNKT, invariant NKT; L-DKO, *Id2^{fl/fl}Id3^{fl/fl}LckCre⁺*; PLZF, promyelocytic leukemia zinc finger; SOM, self-organizing map; SP, single-positive; TKO, *Id2^{fl/fl}Id3^{fl/fl}LckCre⁺CD1d^{-/-}*; WT, wild-type.

Copyright © 2017 by The American Association of Immunologists, Inc. 0022-1767/17/\$30.00

In this article, we describe a rapid generation of iNKT or innate-like lymphoid tumors upon deletion of *Id2* and *Id3* in thymocytes. We also delineate the expanding precursor populations and dysregulated pathways that account for lymphoma development. Given that NKT lymphomas are extremely rare and highly lethal in humans (44), our study provides a much needed animal model for understanding the genetic basis of similar types of tumors in humans.

Materials and Methods

Mice

$Id2^{fl/fl}Id3^{fl/fl}LckCre^+$ (L-DKO) mice were generated as previously described (34). $CD1d^{-/-}$ mice were purchased from the Jackson Laboratory (strain 008881) and were bred with L-DKO mice to generate $Id2^{fl/fl}Id3^{fl/fl}LckCre^+CD1d^{-/-}$ (TKO) mice. All mice were bred in a specific pathogen-free facility at the Duke University Division of Laboratory Animal Resources, and all procedures were performed according to protocols approved by the Institutional Animal Care and Use Committee.

Flow cytometry analysis

Staining with surface marker Abs (BioLegend) was done before intracellular staining for promyelocytic leukemia zinc finger (PLZF) Ab (eBioscience) using a Foxp3 staining buffer set (eBioscience). $CD1dTet^+$ were obtained from the Tetramer Facility of the National Institutes of Health. Flow cytometry analysis was performed on a FACSCanto II (BD Biosciences). Doublets and dead cells (7AAD⁺) were gated out before data analysis. Data were analyzed with FlowJo software (TreeStar).

Histopathological analysis

Tissue sections were removed immediately after sacrificing the mice and fixed in 10% PBS-formalin. Embedding, sectioning, and staining (H&E and Masson's trichrome) were done by the Pathology Service Core at Duke University.

Adoptive transfer of lymphoma cells to $Rag2^{-/-}$ or wild-type hosts

Enlarged thymi from L-DKO donor mice were minced in PBS with 5% bovine calf serum, filtered, lysed for RBCs using BD Pharm Lyse lysing buffer (BD Biosciences), and washed with PBS. A total of 5×10^6 cells per recipient was injected into 6–8-wk-old $Rag2^{-/-}$ mice through their tail vein. Five- to seven-week-old wild-type (WT) mice were sublethally irradiated (300 rad) and injected with tumor cells 24 h later. Recipient mice were sacrificed 4–10 wk after transfer, and tissues were collected for FACS analysis and H&E staining.

PCR and real-time PCR

Genotyping of mice was done as described previously (34). Total RNA was extracted using an RNAqueous kit (Life Technologies), according to the manufacturer's protocol, and reverse transcribed into cDNA using murine leukemia virus reverse transcriptase (Life Technologies). Real time PCR was performed using a FastStart DNA Master SYBR Green Kit, and quantitative expression was normalized to β -actin. The following forward and reverse genotyping primers were used and are listed in 5'–3' orientation: *Id2*^{fl/fl} (forward) 5'-TGTGCATAATTAATCGCATCA-3' and (reverse) 5'-TTGGGAAGTCACATTTGTAGTG-3'; *Id3*^{fl/fl} (forward) 5'-GCTCTGAG-GTCATAAATCCC-3' and (reverse) 5'-CCATTTGGTCTATGTATGCCCG-TG-3'; *LckCre* (forward) 5'-GCAGGAAGTGGGTAAGTACTAGACTAAC-3' and (reverse) 5'-TCTCCCACCGTCAGTACGTGAGATATC-3'; *CD1d* WT (forward) 5'-AGGGCTGTGAGAACTCTGGCGCTA-3' and (reverse) 5'-GCAGGGAGCGGAAGGTGTAATT-3'; and *CD1d* KO (forward) 5'-AGGGCCAGCTCATTCTCCACT-3' and (reverse) 5'-GCAGGGAGCG-GAAGGTGTAATT-3'. The following real time PCR primers were used: *IL-4* (forward) 5'-ATCATCGGCATTTTGAACGAGGTC-3' and (reverse) 5'-ACCTTGGAAGCCCTACAGACGA-3'.

Cell sorting and microarray

Premalignant iNKT cells were sorted as $TCR\beta^+CD1dTet^+$ cells from L-DKO mice at 20 d of age. Lymphoma cells were sorted from tissues of 18–37-wk-old mice as T cells that are $CD1dTet^+$ or $CD1dTet^-$. Total RNA was extracted as described for real time PCR. mRNA expression profiling was done by the Duke Microarray Core Facility using GeneChip Mouse Genome 430A 2.0 arrays (Affymetrix). The microarray data have been submitted to the Gene Expression Omnibus repository under the accession number GSE83761.

Bioinformatics and statistical analysis

Microarray data for premalignant and lymphoma cells were normalized using RMA, and differential analysis was done using the *limma* package available through Bioconductor (45). Publicly available normalized ImmGen data for WT cells were requested and downloaded from <http://rstats.immgen.org/DataRequest/> (46). The two normalized datasets were combined according to the Empirical Bayes method using the Web tool ArrayMining (<http://www.arraymining.net>) (47).

Data plotting, visualization, and statistics

Gene-expression (fold change) heat maps were generated using Gene-E (<http://www.broadinstitute.org/cancer/software/GENE-E/>). Self-organizing maps (SOM) were generated by the Partek Genomics Suite made available by the Duke Center for Genome and Computational Biology. Principal component analysis was performed and plotted using the built-in R functions *prcomp* and *plot3d* in open-source RStudio software. Gene overlaps in the form of a Venn diagram were drawn using eulerAPE software (48). Pathway analysis was done using HOMER software (49). Survival curves and bar graphs were drawn using GraphPad Prism (GraphPad). The two-tailed Student *t* test was used for statistical analyses, with *p* values < 0.05 considered significant.

Results

Conditional deletion of *Id2* and *Id3* leads to rapid lymphoma development

We previously reported a dramatic expansion of iNKT cells upon *Id2/Id3* conditional deletion using *LckCre* in L-DKO mice (34). Surprisingly, we found that these mice also rapidly develop tumors and start dying between 3 and 11 mo of age (Fig. 1A). L-DKO mice developed lymphoma in several organs, including thymus, lymph nodes, bone marrow, spleen, liver, and gut (Table I). Splenomegaly and hepatomegaly were apparent in all mutant mice analyzed in this age window, which also were reflected in the significant increase in the weight of liver and spleen of these mice compared with control mice (Fig. 1B). Histopathological H&E staining of the thymus, spleen, liver, lung, and kidney of L-DKO tumor mice revealed infiltration of lymphoma cells in these organs, as well as the disruption of normal tissue structures (Fig. 1C). Masson's trichrome staining, which is used to detect collagen and fibrosis in tissues, suggested a mild fibrosis in the lymphoma-infiltrated area of livers of L-DKO mice aged ≥ 5 mo (Fig. 1D). At this stage, the normal liver parenchyma was replaced by malignant lymphocytes, which could also lead to liver dysfunction and death. Thus, we observed that conditional deletion of *Id2* and *Id3* led to lymphocyte infiltration and rapid development of tumors in various peripheral organs, which ultimately caused their death.

L-DKO lymphomas are derived from $CD1dTet^+$ iNKT cells or $CD1dTet^-$ innate-like T cells

Because we previously observed neonatal expansion of iNKT cells in L-DKO mice, we hypothesized that the tumors in these mice are derived from the uncontrolled expansion of the iNKT cell population. However, upon further assessment, we found that only 36% of L-DKO mice developed $CD1dTet^+TCR\beta^+$ tumors, whereas the rest primarily developed $CD1dTet^-TCR\beta^+$ tumors (Fig. 2A, Table I).

A recent publication from Cornelis Murre's group has also described the expansion of innate-like follicular helper T cells and lymphoma development in $Id2^{fl/fl}Id3^{fl/fl}IL7RCre$ mice (50). To better characterize the lymphoma populations in L-DKO mice (with a later deletion of *Id2/Id3*), we started by examining the expression of PLZF, a key transcription factor for all innate-like cells, including iNKT cells (29, 51). High PLZF expression in the $CD1dTet^+TCR\beta^+$ population verified that these were indeed NKT cells (Fig. 2B, upper panels). The NKT lymphoma cells were further confirmed to be iNKT cells by their typical $V\alpha14J\alpha18$ rearrangement, which was not observed in $CD1dTet^-$ cells

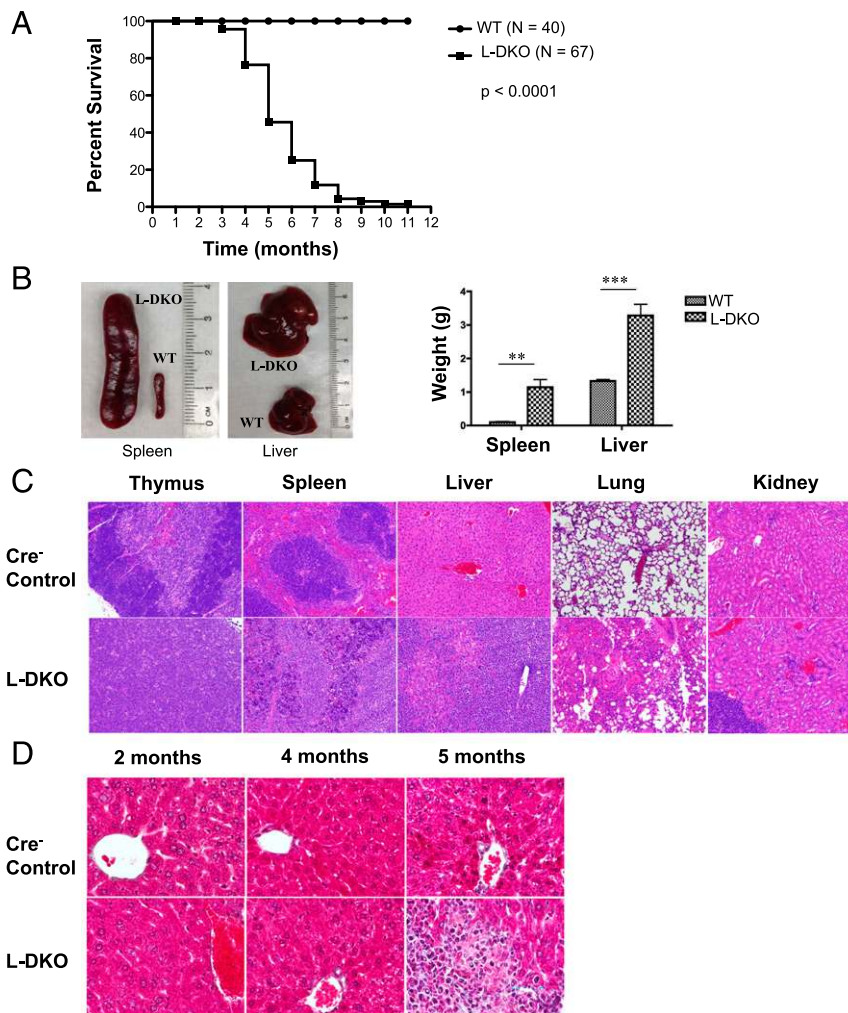


FIGURE 1. Deficiency of both Id2 and Id3 in developing T cells leads to lymphomagenesis in mice. **(A)** Survival curve for L-DKO and control (LckCre⁻) mice. The p value was determined using the Mantel–Cox test. **(B)** Comparison of size and weight of spleen and liver from L-DKO ($n = 5$) and WT control ($n = 4$) mice. **(C)** Representative H&E staining for thymus, spleen, liver, lung, and kidney from L-DKO mice and controls (original magnification $\times 100$). **(D)** Representative Masson's trichrome staining for livers from L-DKO mice and controls at 2, 4, and 5 mo of age (original magnification $\times 400$). $n = 3$ for (C) and (D). ** p value between 0.001 and 0.01, *** p value between 0.0001 and 0.001.

(Fig. 2C). Interestingly, CD1dTet⁻TCR β ⁺ cells also were found to be PLZF⁺, distinguishing them from conventional $\alpha\beta$ T cells (Fig. 2B, lower panels). Phenotypic analysis of tumor samples from several L-DKO tumor mice also revealed that the majority of lymphoma cells (both CD1dTet⁺ and CD1dTet⁻) expressed the surface markers CD69 and CD44 but lacked CD25 and CD24 expression, similar to innate-like iNKT cells (Table I). These expression patterns further verified that the PLZF⁺CD1dTet⁻TCR β ⁺ population was innate-like. Although other groups of investigators also reported the expansion of PLZF⁺CD1dTet⁻TCR β ⁺ populations in the absence of Id proteins, the different stage of *Id* deletion and lack of comprehensive surface markers make these populations difficult to compare (52, 53). Thus, we found that L-DKO mice develop innate-like T cell lymphomas that are derived from CD1dTet⁺ iNKT cells or CD1dTet⁻ innate-like T cells.

Malignant innate-like T cells from L-DKO mice are able to invade healthy tissues

To evaluate the tumorigenic potential of innate-like lymphoma cells in L-DKO mice, we transferred these cells into Rag2^{-/-} mice. We found that 70% of the Rag2^{-/-} recipients died within 7–12 wk of transfer of L-DKO lymphoma cells (Fig. 3A). Substantial lymphocyte infiltration was observed by H&E staining of liver and spleen tissues from recipient mice (Fig. 3B). It was also evident that CD1dTet⁺ cells and CD1dTet⁻ cells were capable of giving rise to secondary lymphomas in Rag2^{-/-} hosts. These secondary lymphomas matched the original phenotype of the

donor innate-like lymphoma cells, such that lymphomas derived from donor 1 cells were CD1dTet⁺PLZF⁺, whereas those from donor 2 gave rise to CD1dTet⁻PLZF⁺ lymphomas (Fig. 3C). Adoptive transfer of lymphoma cells into WT hosts also gave rise to tumors within 10 wk (Supplemental Fig. 1), indicating that these tumors acquire the ability to evade immune surveillance. These results demonstrated the malignancy of these innate-like lymphomas derived from L-DKO mice.

CD1dTet⁻ innate-like T cells start expanding in neonatal L-DKO mice

Next, we wanted to explore the possible neonatal expansion of these cells in L-DKO mice, similar to iNKT cells. After gating out $\gamma\delta$ T cells, which aberrantly upregulate CD4 and CD8 in L-DKO mice, we found that the CD1dTet⁻TCR β ⁺ population was indeed expanded in 20-d-old L-DKO mice (Fig. 4A). This population had markedly upregulated PLZF expression, clearly demarcating them from conventional CD4 single-positive (SP) and double-negative (DN) cells. Interestingly, the PLZF level in CD4 SP CD1dTet⁻ cells was even higher than that in iNKT cells. Compared with WT conventional CD4 T cells, we found that innate-like CD4⁺CD1dTet⁻ cells had a lower surface expression of TCR β and CD24 that was similar to iNKT cells from L-DKO mice (Fig. 4B). We also looked at surface expression of CD122 and CD25, which are usually upregulated in type II NKT cells. However, we found no significant upregulation of these markers among the L-DKO CD1dTet⁻ population (Fig. 4B). These cells had a broader and more evenly spread TCR β usage than did CD1dTet⁺ iNKT cells,

Table I. Phenotypic characteristics of tumors in L-DKO mice

Original Tumor				T Cell Markers			Other Markers for TCRβ ⁺ Cells				
No.	Sex	Age (wk)	Involvement	TCRβ	CD4	CD8	CD1dTet	CD44	CD25	CD24	CD69
LII10 ^a	F	19	T S L G	+	34%	–	–	ND	ND	ND	ND
LII30	M	27	T S L	+	78%	–	+	ND	ND	ND	ND
LIII10	M	18	T S L G	+	43%	–	–	int	–	–	ND
L60	M	26	T S L	+	79%	9%	+	int	–	int	ND
LIII22	F	27	T S L LN BM	+	41%	46%	–	int	–	–	+
LII65	M	25	T S L BM	10%	10%	–	+	int	–	–	ND
LII66	M	25	T S L	5%	–	–	+	int	–	–	ND
LIII36	F	30	T S L LN BM	+	31%	42%	–	int	–	–	ND
LIII46	F	27	T S L LN BM	+	–	78%	+	int	–	–	ND
LVI 23	M	24	T S L G LN BM	+	–	–	+	int	–	–	ND
LV9	M	20	T S L G	+	49%	–	–	int	–	–	ND
LVI 7 ^b	F	33	T S L G LN BM	+	–	58%	–	int	–	–	ND
LV27 ^a	M	25	T S L LN BM	+	–	–	–	int	–	–	+
LV40	M	29	T S L G LN BM	+	90%	–	–	int	–	–	+
LV69 ^b	F	26	T S L G LN BM	+	43%	–	–	int	–	–	+
LIV9	M	29	T S L LN BM	+	78%	–	–	int	–	–	+
LIV11	M	29	T S L G BM	+	84%	–	–	int	–	–	+
LV36	F	34	T S L G LN BM	+	92%	–	–	int	–	–	+
LIV34 ^c	M	20	T S L G LN BM	+	82%	–	+	int	–	int	+
LIV56	F	18	T S L G LN BM	+	46%	–	+	int	–	–	+
LV21 ^c	M	37	T S L G LN BM	+	70%	20%	–	int	–	int	+
LIII5 ^a	F	18	T S L G	+	70%	–	–	int	–	–	+
LIII12 ^a	F	18	T S L G LN BM	+	31%	49%	–	int	–	–	+
LIII10 ^{a,c}	M	20	T S L G LN BM	+	20%	–	+	int	–	–	+
LIII14 ^b	M	20	T S L LN BM	+	75%	–	–	int	–	–	+
LIII57 ^{a,c}	M	20	T S L G LN BM	+	36%	–	+	int	–	–	+
LIII75 ^{a,b,c}	M	19	T S L G LN BM	+	23%	32%	–	int	–	int	+

^aMice with lymphocyte-infiltrated lung.

^bMice with lymphocyte-infiltrated kidney.

^cMice with lymphadenopathy.

–, negative; +, positive; BM, bone marrow; F, female; G, gut; int, intermediate; L, liver; LN, lymph node; M, male; S, spleen; T, thymus.

which is more typical of type II NKT cells (Fig. 4C). A unique feature of innate-like lymphocytes is their ability to produce IL-4 in the steady-state. Quantitative PCR analysis revealed that the CD4⁺CD1dTet[–] population had a higher expression of IL-4 in the steady-state compared with iNKT cells and conventional CD4 T cells, which indicated a possible regulatory role for this subset (Fig. 4D). These observations are indicative of neonatal expansion of the innate-like CD1dTet[–] population, which has shared features with type II NKT cells.

CD1dTet[–] cells develop in a CD1d-independent manner and expand to cause lymphoma in L-DKO CD1d-deficient mice

Because we found low expression of CD122 and CD25 but a diverse TCRβ repertoire among L-DKO CD1dTet[–] cells, we needed to further verify whether the L-DKO CD1dTet[–] cells belonged to the type II NKT lineage. It is known that all types of αβ NKT cells depend on CD1d-mediated selection for their development (54). Therefore, we generated TKO mice and found that the CD1dTet[–]TCRβ⁺ population was still existent in the absence of *CD1d* (Fig. 5A). PLZF expression also verified that CD1d[–]TCRβ⁺ cells in TKO mice were innate-like (Fig. 5B). TCRα repertoire analysis indicated that CD1dTet[–]TCRβ⁺ cells from TKO and L-DKO mice had fairly broad distribution of TCRα chains, with no clear preference for Vα14 or Vα3, unlike iNKT cells and type II NKT cells (Fig. 6A). Similar TCRβ usage also suggested that the same CD1dTet[–] population was present in TKO and L-DKO mice (Figs. 4C, 6B). Interestingly, one of the TKO mice demonstrated a dominant usage of Vβ7, which suggested possible clonal expansion and tumorigenic potential as early as 20 d of age. Cumulatively, these data verified that these CD1dTet[–] cells are innate-like and a novel type of CD1d-independent NKT cell, similar to γδ NKT cells. We found

that lymphocyte infiltration by the expanded CD1dTet[–] population also gave rise to tumors in TKO mice (Supplemental Fig. 2).

Neonatal L-DKO iNKT cells have a unique transcriptional program that promotes NKT cell development and expansion and predisposes them to lymphomagenesis

We next sought to identify the dysregulated molecular mechanisms responsible for tumor initiation and development. We did a microarray analysis to compare premalignant iNKT cells from 20-d-old L-DKO mice and lymphoma cells (CD1dTet[–] or CD1dTet⁺/iNKT in origin) from L-DKO mice with well-developed tumors. We found that the tumors upregulated several genes and downregulated fewer genes compared with premalignant iNKT cells (Fig. 7A). Hierarchical clustering also demonstrated a clear distinction between lymphoma and premalignant iNKT cells, as well as more variability between the tumor samples (Fig. 7A). To allow direct comparisons of our L-DKO premalignant and tumor cells with control WT NKT cells and WT double-positive (DP) cells, we combined our microarray data with publicly available ImmGen data (46). Clustering patterns showed clear segregation among the WT NKT, L-DKO neonatal, and tumor samples (Fig. 7B, 7C). We found that there were both shared and unique gene signatures among WT NKT cells, premalignant L-DKO iNKT cells, and CD1dTet⁺ NKT tumors; surprisingly, there was only a moderate overlap between 20-d L-DKO NKT cells and WT NKT cells (Fig. 7B, 7D).

Based on the expression patterns of gene clusters in the samples, we identified genes that were differentially expressed in WT or L-DKO iNKT cells (Fig. 7B, Supplemental Table I). Interestingly, a significant fraction of genes were downregulated in L-DKO iNKT cells compared with WT NKT cells, which included anti-proliferative and proapoptotic genes *Pawr* (55) and *Lgals1* (56) and tumor-suppressor genes *Cebpb* (57) and *Irf5* (58) (Fig. 7E).

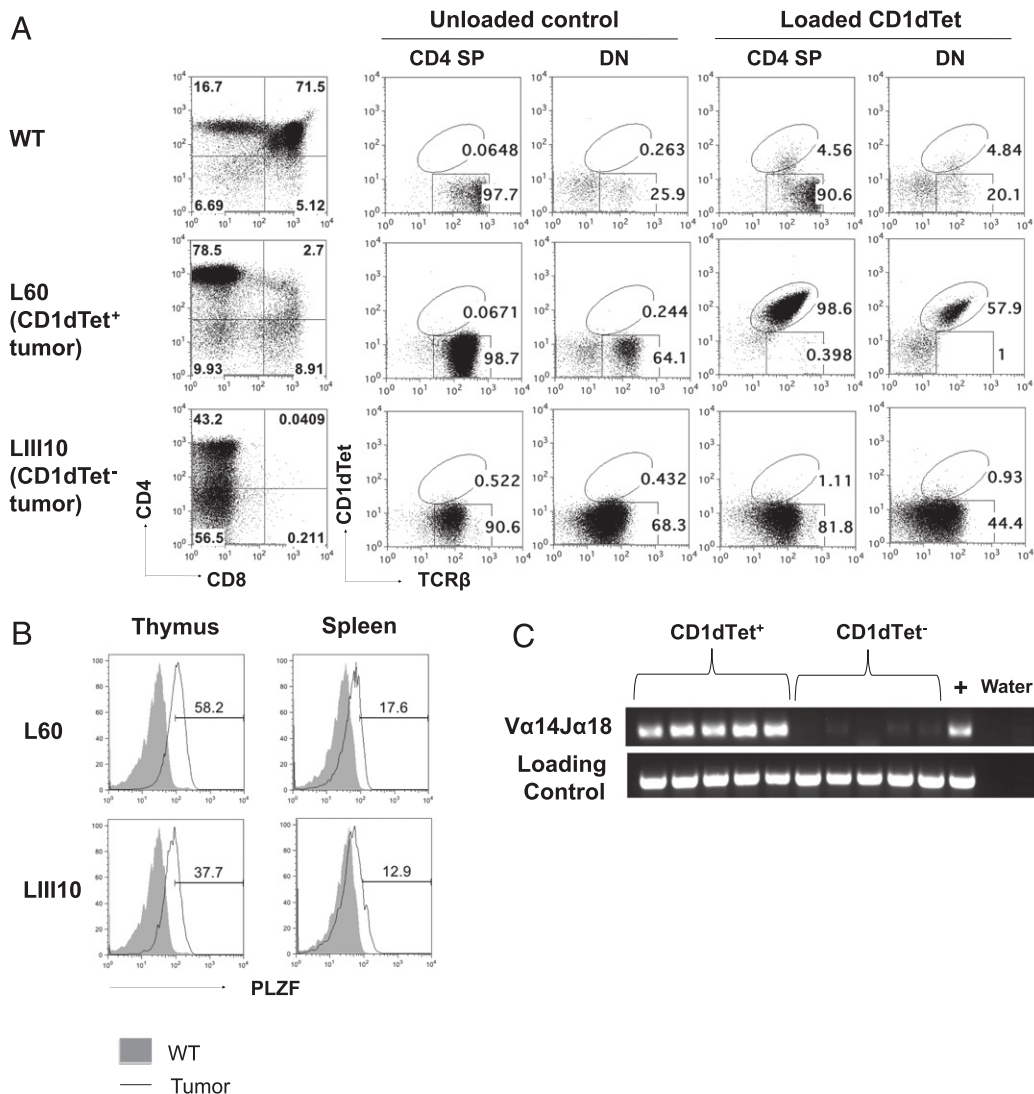


FIGURE 2. Lymphomas in L-DKO mice are CD1dTet⁺ (iNKT) or CD1dTet⁻ in origin. **(A)** Representative staining of thymocytes with CD4 and CD8 markers from a Cre⁻ control and two L-DKO mice with CD1dTet⁺ (L60) or CD1dTet⁻ (LIII10) tumor. CD4 and DN fractions were analyzed further by staining with TCRβ and CD1dTet without or with loaded Ag. **(B)** Representative graphs of intracellular PLZF staining of TCRβ⁺ populations from mice ($n = 2$) with tumor shown in (A). **(C)** Detection of Vα14Jα18 rearrangement in CD1dTet⁺ or CD1dTet⁻ lymphoma samples by PCR. CD14 was used as a loading control ($n = 5$).

Genes implicated in cell cycle progression and metastasis, such as *Vangl2* (Wnt pathway), *Cdk1* (p53 pathway), *Ccr7*, and *Igfbp4*, were significantly upregulated in L-DKO iNKT cells. *Dgka*, which was reported to be important for NKT cell development (59), as well as for promoting tumorigenesis (60), was also found to be upregulated >2-fold in L-DKO iNKT cells. These expression patterns supported the tumorigenic potential of these cells.

In contrast, these premalignant cells also demonstrated the upregulation of several cell cycle arrest, tumor-suppressor, and antiproliferative genes, such as *Rprm* (61), *Ptpn14* (62), and *Btg2* (63) (Fig. 7E). Other genes that commonly contribute to tumor development or are overexpressed in tumors, such as *Pkd2* (64), *Mmp2* (65), *Adm* (66), and *Vcam1* (67), had reduced expression in these cells. Genes involved in cytokine–cytokine receptor interaction, many of which were implicated in facilitating tumor metastasis, were also downregulated (Fig. 7F) (68). These data hint toward the existence of a tumor-suppression program in these cells that prevents tumorigenesis at this stage.

Rag2 was found to be upregulated >3-fold in L-DKO iNKT cells, which would allow prolonged TCRα rearrangement

to increase chances of the distal Vα14Jα18 rearrangement to promote iNKT cell development (Fig. 7E) (69). We previously described a block in iNKT development beyond stage 1 in L-DKO mice, which allows these cells to constantly proliferate without undergoing maturation (34). We found downregulation of *Relb* in L-DKO iNKT cells, which was described as being critical for the developmental progression of NKT cells to stages 2 and 3 (70). Overall, gene expression and pathway analysis revealed that *Id2/Id3* deletion initiates a modified transcriptional program in L-DKO iNKT cells that supports their prolific expansion while maintaining a premalignant state.

Conditional *Id2/Id3* deletion promotes acquisition of multiple tumorigenic programs

Because the tumors in L-DKO mice share lineage identity with iNKT cells or CD1dTet⁻ cells that had undergone persistent expansion starting at a neonatal age, it is likely that the acquisition of secondary and tertiary oncogenic mutations ultimately led to tumor development. We found a clear distinction between the tumor samples that could indicate the existence of multiple, varying

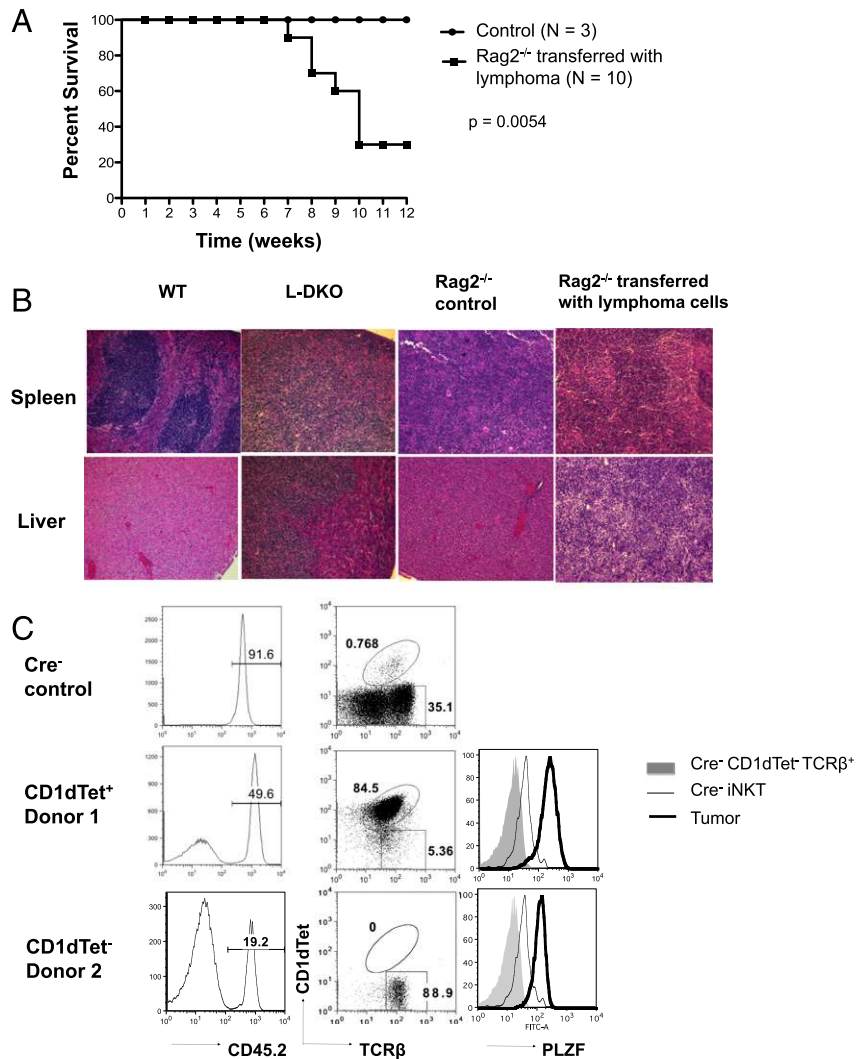


FIGURE 3. Adoptive transfer of L-DKO lymphoma cells gives rise to tumor in *Rag2*-deficient recipients. **(A)** Survival curve for *Rag2*^{-/-} hosts after receiving 5×10^6 lymphoma cells from L-DKO mice ($n = 10$). *Rag2*^{-/-} mice that were not injected with lymphoma cells were used as control ($n = 3$). The p value was determined using the Mantel–Cox test. **(B)** Representative H&E staining for spleen and liver from WT control, L-DKO mice with lymphoma, *Rag2*^{-/-} control, and *Rag2*^{-/-} mice that received lymphoma cells ($n = 5$ for each host type). Original magnification $\times 100$. **(C)** CD45.2⁺ lymphoma cells in recipient mice analyzed for their CD1dTet and TCR β expression. Intracellular PLZF expression levels in CD1dTet⁻TCR β ⁺ and CD1dTet⁺TCR β ⁺ (iNKT) control cells from Cre⁻ mice and CD45.2⁺ tumor cells from *Rag2*^{-/-} recipients. Data are representative of three analyzed recipients.

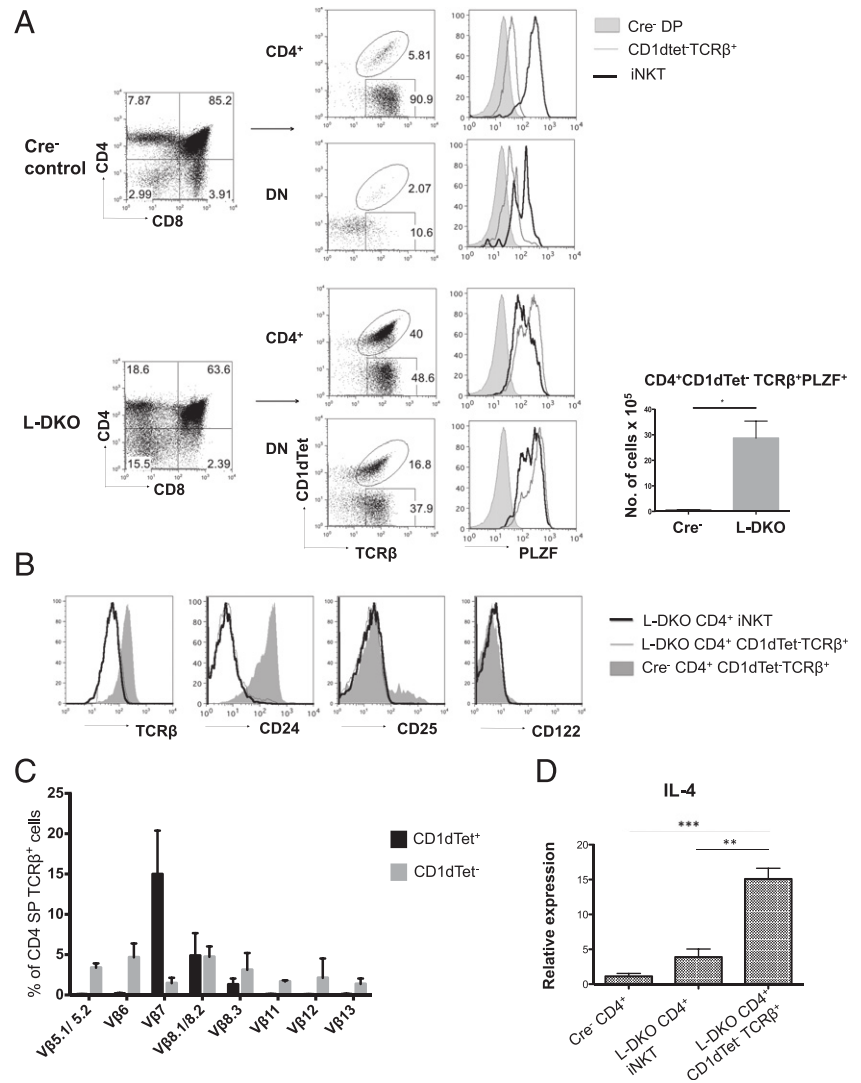
aberrant pathways that are reflective of the history of accumulated mutations in the parent cells, which was also supported by their oligoclonal expansion patterns (Fig. 7C). Karyotyping analysis of lymphoma cells from L-DKO mice also revealed aneuploidy in one of two tumor cases (Supplemental Fig. 3). This could be an indication of chromosome instability, which is often linked to tumorigenesis, and may play a role in promoting lymphoma development in L-DKO mice (49, 71).

Because the CD1dTet⁻ tumor sample was significantly distant from CD1dTet⁺ tumors, it was treated as a unique outlier and was not analyzed further. We then focused our attention on iNKT cell tumor samples and identified genes with >2 -fold expression in L-DKO iNKT cells, iNKT tumors, or WT NKT cells compared with WT DP cells (Fig. 7D). Of these genes, iNKT tumor cells had a largely unique gene profile, with only a small fraction retained in common with WT NKT cells and premalignant L-DKO iNKT cells. We also performed pathway analysis to identify the pathways overrepresented in the tumor samples (Fig. 8A) (49). This analysis revealed many aberrant pathways specific to the tumor samples, particularly corresponding to cytokine–cytokine receptor interaction, NF- κ B signaling, and transcriptional misregulation in cancer (Fig. 8A, 8B). Interestingly, the cytokine–cytokine receptor pathway, which was downregulated in premalignant iNKT cells, was found to be upregulated upon tumorigenesis. This included genes (*Csf1r*) that aid in proliferation and can act as proto-oncogenes (72), as well as chemokines and their ligands (*Cxcl12*, *Ccl11*, *Ccl9*, *Ccr1*,

Ccr5) that contribute to metastasis (73, 74). We noted that upregulation of *Csf1r* was uniquely detected in iNKT cell lymphomas but not in CD1dTet⁻ lymphomas (Fig. 8C). *Icam1* and *Cxcl12*, which are reported to regulate NKT cell homing to the liver and bone marrow (75, 76), were also upregulated in the tumor cells and, therefore, could potentially promote accumulation of iNKT cells and tumor formation (77, 78) in these organs (Table I). *Lta* and *Ltb* are known to play roles in iNKT thymic emigration (79) and were significantly upregulated in iNKT tumors. Furthermore, several interesting genes were involved in the transcriptional misregulation of cancer, such as *Runx2*, *Mmp3*, *Mmp9*, *Egln3*, and *Vegfa* (80–83). We also found upregulation of the *Id2* transcript in iNKT tumors compared with premalignant iNKT cells (Fig. 8B). This could represent overexpression of *Id2* exon 3, which is the only remaining exon in *Id2*^{f/f} mice (84).

We then identified interesting genes that were unique to L-DKO iNKT or iNKT tumor samples (Fig. 8D). Genes supporting cell proliferation, such as *Cd74* (85) and *Adm* (66), were downregulated in premalignant iNKT cells but were highly upregulated in iNKT tumors. The tumor suppressor, *Pcgf2* (86), was also significantly downregulated in iNKT tumor cells. Interestingly, *Ccr7* (87) and *Egr2* (88, 89), which were shown to play critical roles in NKT development, were specifically upregulated in premalignant iNKT cells. Therefore, gene-expression profiling revealed several known oncogenic pathways that may contribute to the development of iNKT tumors. This analysis also indicated that there were

FIGURE 4. Innate-like CD1dTet⁻ T cells expand in the absence of Id2 and Id3. **(A)** Representative flow cytometry analysis of thymocytes (TCR $\gamma\delta^+$ cells gated out) from 20-d-old L-DKO and Cre⁻ control mice. Cells were stained for CD4 and CD8 to separate the CD4⁺ and DN populations, which were further analyzed with TCR β and CD1dTet markers. Intracellular PLZF staining is shown for the corresponding CD1dTet⁻ and CD1dTet⁺ (iNKT) cells from the CD4 SP and DN fractions, along with Cre⁻ DP cells as controls. Absolute numbers of CD4⁺CD1dTet⁻TCR β^+ PLZF⁺ cells for 20-d-old L-DKO and Cre⁻ mice ($n = 3$ for each). **(B)** Representative surface staining of thymocytes gated on CD4⁺CD1dTet⁺ (iNKT) or CD4⁺CD1dTet⁻TCR β^+ cells from 20-d-old L-DKO or Cre⁻ control mice. Graphs show TCR β , CD24, CD25, and CD122 staining ($n = 2$). **(C)** TCR β -chain distribution among CD4⁺TCR β^+ CD1dTet⁺ (iNKT) or CD4⁺TCR β^+ CD1dTet⁻ cells from 20-d-old L-DKO and Cre⁻ controls ($n = 4$), as measured by a panel of corresponding V β Abs. **(D)** IL-4 transcript expression in sorted CD4⁺TCR β^+ CD1dTet⁺ (iNKTs) and CD1dTet⁻ cells from 20-d-old Cre⁻ and L-DKO mice, as measured by real time PCR ($n = 4$). ** p value between 0.001 and 0.01, *** p value between 0.0001 and 0.001.



distinct pathways involved in the premalignant expansion of iNKT cells and the ultimate transformation of iNKT cells leading to uncontrolled tumor growth (Fig. 8E). However, comparison of

these identified genes and pathways revealed only a limited overlap with the lymphomas described in Id2^{fl/fl}Id3^{fl/fl}IL7R^{Cre} mice (data not shown). We also found a moderate, but varying,

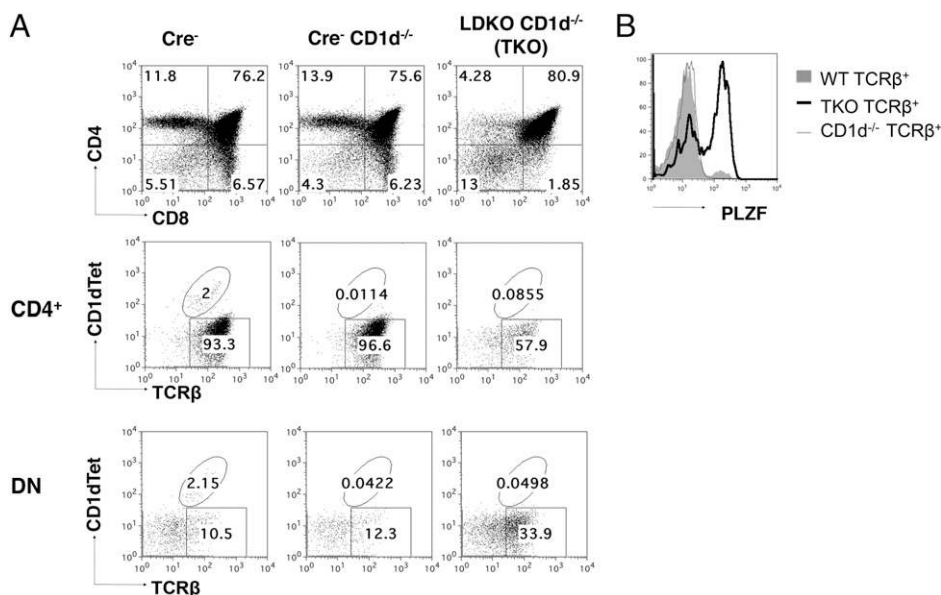


FIGURE 5. Expansion of CD1d-independent innate-like T cells in TKO mice. **(A)** Representative staining of thymocytes from 20-d-old Cre⁻ control, Cre⁻ CD1d^{-/-} control, or L-DKO CD1d^{-/-} (TKO) mice using CD4 and CD8 markers (top panels). CD4⁺ and DN gated cells were further analyzed for CD1dTet and TCR β expression. **(B)** Representative intracellular PLZF staining for TCR β^+ cells from 20-d-old WT (Cre⁻), Cre⁻ CD1d^{-/-}, and TKO mice ($n = 3$).

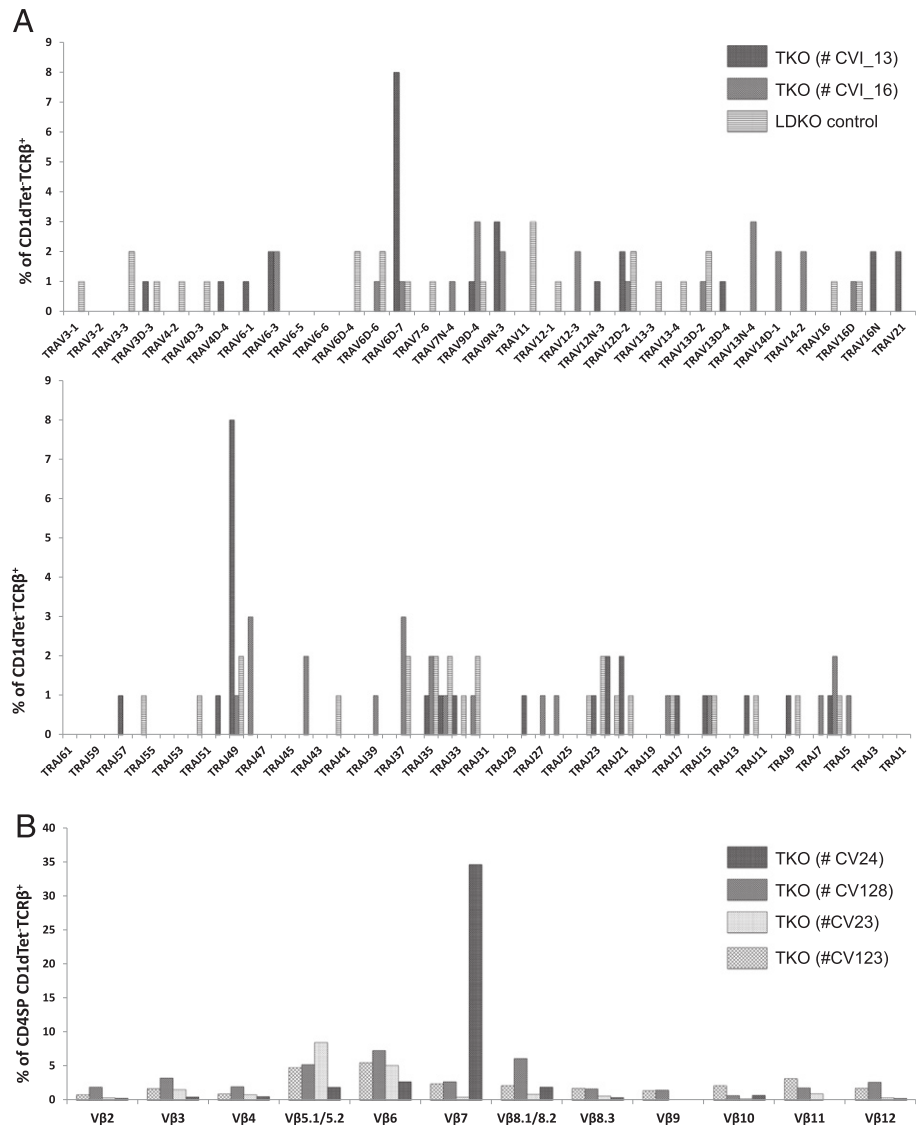


FIGURE 6. CD1d-independent CD1dTet⁻ TCRβ⁺ T cells have broad TCRα and TCRβ repertoires. **(A)** Vα and Jα repertoires (percentage usage) of CD1dTet⁻ TCRβ⁺ T cells from 20-d-old TKO mice ($n = 2$) and L-DKO ($n = 1$) mice, as measured by 5'RACE (Invitrogen). TRAV11 and TRAV9 correspond to Vα14 and Vα3 chains, respectively, according to the new HUGO Gene Nomenclature Committee. **(B)** TCRβ-chain distribution among CD4⁺TCRβ⁺CD1dTet⁻ cells from 20-d-old TKO mice ($n = 4$), as measured by a panel of corresponding Vβ Abs. Repertoire for each individual mouse is depicted by a separate pattern.

upregulation of CXCR5 in L-DKO lymphoma cells (data not shown) (50). The phenotypic difference between NKT tumors in L-DKO mice and follicular helper T cell tumors in $Id2^{fl/fl}Id3^{fl/fl}$ IL7R^{Cre} mice indicates that tumor types may be dictated by the timing of Id gene deletion.

Additionally, to determine similarity with human NKT tumors, we compared our L-DKO tumor data with a recent publication characterizing key driver mutations and pathways in patients with NKT lymphomas (90, 91). We found that many of the mutated genes in human patients from their study (90) were also dysregulated in the L-DKO tumor model. The shared genes had differential expression patterns in L-DKO iNKT tumor samples and neonatal iNKT cells compared with WT NKT cells (Fig. 8F). The article also implicated upregulation of the NF-κB pathway in driving tumorigenesis in a subset of patients with poor prognosis (90). Several genes of the NF-κB pathway also were found to be uniquely upregulated or downregulated in L-DKO iNKT tumors but not in premalignant neonatal iNKT cells (Fig. 8B). These data suggest that this is a potential mouse model to investigate mechanisms of iNKT and innate-like tumors in humans.

Discussion

A previous study of $Id3^{-/-}$ mice revealed a tumor-suppressor role for Id3 in the development of hepatosplenic T cell lymphoma-like

tumors (20). In this study, we observed iNKT cell and innate-like T cell tumors upon deletion of both *Id2* and *Id3*. It is interesting to note the difference in the kinetics of lymphoma development and progression in $Id3^{-/-}$ mice and L-DKO mice. $Id3^{-/-}$ mice often develop autoimmune diseases (92), but tumor development is much more infrequent and delayed, such that these mice live for ≥ 1 y. In contrast, L-DKO mice start dying of tumor by 3 mo of age. This rapid development of αβ T cell lymphomas in $Id2^{fl/fl}Id3^{fl/fl}IL7R^{Cre+}$ mice (50) and iNKT cell and CD1dTet⁻ tumors in L-DKO mice argue in favor of Id2 playing novel compensatory and nonredundant roles, together with Id3, in the regulation and suppression of tumorigenesis of developing T cells in the murine thymus.

Previous reports demonstrated a role for Id proteins in suppressing the development of innate-like γδ and iNKT cells (29, 35). Our findings highlight the suppressive role of Id proteins in overall innate-like T cell development, such that there is also expansion of CD1dTet⁻ innate-like T cells in L-DKO mice. Interestingly, this population bears a resemblance to the CD4⁺ PLZF⁺ cells that expand in mice deficient in *Itk* or *Id3* or with early deletion of both *Id2* and *Id3* (50, 52, 93). Additional characterization of surface markers and gene-expression programs in these cells would be important for comparing these innate-like T cells and for understanding the cellular origin of iNKT and innate-like T cell tumors in humans (44, 48, 94, 95).

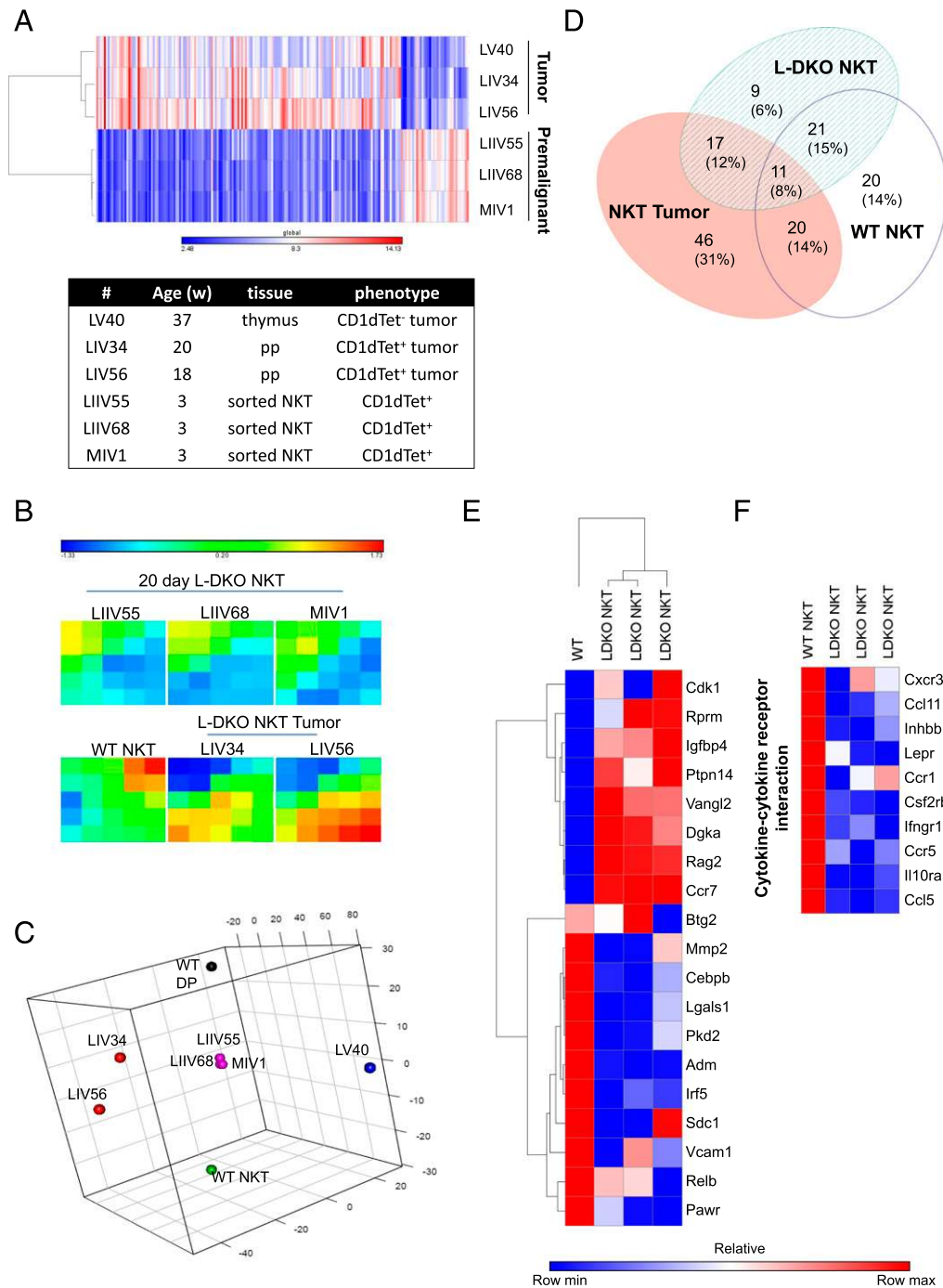


FIGURE 7. Aberrant gene-expression program in neonatal NKT cells in the absence of *Id2* and *Id3*. **(A)** Heat map with hierarchical clustering showing gene expression in sorted neonatal NKT cells from 20-d-old L-DKO mice and tumor cells (CD1dTet⁺ and CD1dTet⁻) from 18- to 37-wk-old mice, as measured by mouse genome arrays. Colors represent global values of low (blue) to high (red) gene expression, with values ranging from 2.48 to 14.13 (in log₂ scale, normalized values). Age of the mice, tissue origin of cells, and their phenotype are also listed. **(B)** SOM showing gene expression in clusters of genes for tumor or NKT cells from mice listed above or from WT control mice (combined data). Colors represent low (blue) to high (red) log₂ fold change in gene expression with respect to WT DP cells. **(C)** Principal component analysis for L-DKO NKT, NKT tumor, and CD1dTet⁻ tumor samples [described in (A)], combined with WT NKT and WT DP cells from ImmGen. **(D)** Venn diagram represents the number and percentage of NKT-specific genes ($p < 0.05$ and absolute fold change > 2 in WT NKT cells with respect to WT DP cells) that are unique or shared among WT NKT, neonatal L-DKO NKT, and NKT tumor cells. **(E)** Heat map showing hierarchical clustering and relative log fold change of gene expression in WT NKT and neonatal L-DKO NKT cells with respect to WT DP cells. Genes were selected based on expression patterns of SOM clusters (listed in Supplemental Table I). **(F)** Heat map showing the relative log fold change for genes involved in cytokine-cytokine receptor interaction. For (E) and (F), colors represent the lowest (blue) to highest (red) fold change of a particular gene among the different samples.

To delve into the mechanism(s) of tumor formation in L-DKO mice, we performed a meta-analysis by combining our L-DKO microarray data with WT data. This allowed us to perform direct comparisons between our mutant cells and WT NKT cells,

which were originally not included in our microarray analysis. However, this approach limits the analysis to only the common gene probes in the two microarray datasets, which can lead to the omission of some potentially interesting genes in this model. It is

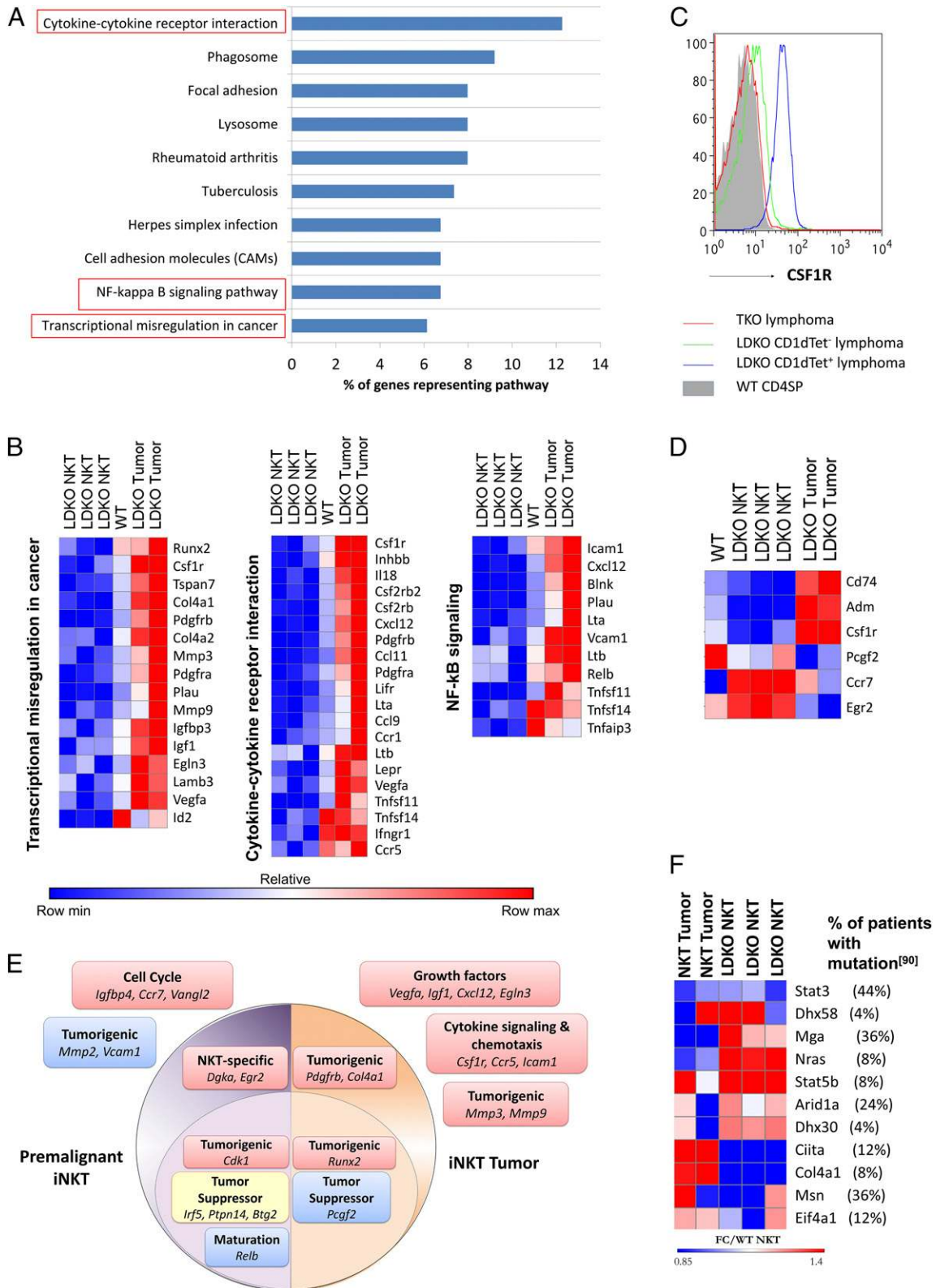


FIGURE 8. The concurrent loss of Id2 and Id3 turns on an oncogenic program in NKT cells. **(A)** Pathways overrepresented by genes with >2-fold gene expression in NKT tumor samples according to gene sets annotated by Kyoto Encyclopedia of Genes and Genomes (96). Percentages represent the fraction of genes from each pathway that are overexpressed in the samples. **(B)** Heat maps showing relative log fold change in gene expression with respect to WT DP cells for genes from pathways identified in the above analysis. **(C)** Representative CSF1R surface staining for CD1dTet⁺, CD1dTet⁻ lymphoma samples (*n* = 4) from L-DKO, TKO, and WT control mice (*n* = 3). **(D)** Heat maps showing select genes with significant differential expression among premalignant and tumor samples. **(E)** Graphic depicting a few key overrepresented pathways in premalignant NKT cells from 20-d-old L-DKO mice (purple) or in CD1dTet⁺ NKT lymphoma cells from older L-DKO mice (orange). Downregulation (blue), upregulation (red), or partial upregulation and downregulation (yellow) of selected genes from the pathways are also shown. **(F)** Fold change in gene expression, with respect to WT NKT cells, of genes that are implicated in human NKT tumors (90) and also dysregulated in L-DKO iNKT tumors. Percentages refer to patients with NKT lymphomas (total *n* = 25) who have mutations in the listed genes, as characterized by Jiang et al. (90).

also important to note that the expanded iNKT cells in L-DKO mice are a heterogeneous population consisting primarily of stage 1 and stage 2 NKT cells (34). Because of the lack of availability of an appropriate control population, we used mature NKT cells from B6 mice as reference. Despite this distinction between the populations, it is reasonable to make this comparison as a reflection of changes in transcriptional programs in NKT cells lacking *Id2* and *Id3* that lead to lymphoma development. With the microarray datasets combined, we were able to observe the deviation in the genetic program in L-DKO iNKT cells compared with WT NKT cells. We found that several cell cycle genes were upregulated and proapoptotic genes were downregulated in neonatal L-DKO iNKT cells. This modified program allowed their dramatic expansion but also kept their tumorigenic potential in check. We inferred that these expanding neonatal innate-like cells are stochastically driven toward tumorigenesis via different pathways, giving rise to heterogeneous tumors in these mice.

Among L-DKO tumors, we observed dysregulation of genes in several pathways, such as transcriptional misregulation in cancer and cytokine–cytokine receptor interactions, as well as others that are commonly overexpressed in various cancer types. Although it is difficult to determine with certainty which genes contributed to lymphoma development versus those that were upregulated as a result of lymphoma development, we verified the sharing of key genes and pathways in L-DKO tumors and human NKT tumors. Therefore, these mice serve as an appropriate mouse model to study iNKT and innate-like tumors. Furthermore, the striking resemblance between all premalignant NKT samples and the divergence of tumor samples leads us to the enticing prospect of treating tumors by identifying and targeting early tumorigenic pathways. Such a study of tumor initiation and gradual progression is only possible in a mouse model and would be useful in determining common genes that lead to malignant transformation.

It is indeed an interesting proposition that *Id2* and *Id3*, through their suppression of innate-like cell fate, prevent unchecked expansion of iNKT cells and CD1d^{hi}Tet⁺ cells under WT conditions. Therefore, upon deletion of *Id2* and *Id3*, the rapid proliferation and expansion of these cells makes them prone to accrual of additional mutations leading to tumorigenesis by various mechanisms.

Acknowledgments

We thank Dr. A. Lasorella and Dr. A. Iavarone (Columbia University) for sharing the *Id2*^{fl/fl} strain. We thank M. Dai (Duke University) for technical assistance with generating the initial L-DKO breeding colony and adoptive transfer of lymphoma cells, the Duke Cancer Center Flow Cytometry Facility for assistance with cell sorting, the Duke Cancer Center Sequencing Facility for assistance with ion torrent sequencing, and the National Institutes of Health Tetramer Core Facility for providing CD1d^{hi}Tet. We thank S. Sen (Carnegie Mellon University) for assistance with bioinformatics analysis and R implementation.

Disclosures

The authors have no financial conflicts of interest.

References

- Hanahan, D., and R. A. Weinberg. 2011. Hallmarks of cancer: the next generation. *Cell* 144: 646–674.
- Hainaut, P., and A. Plymoth. 2013. Targeting the hallmarks of cancer: towards a rational approach to next-generation cancer therapy. *Curr. Opin. Oncol.* 25: 50–51.
- Ellenbroek, S. I., and J. van Rheenen. 2014. Imaging hallmarks of cancer in living mice. *Nat. Rev. Cancer* 14: 406–418.
- Evan, G. I., and K. H. Vousden. 2001. Proliferation, cell cycle and apoptosis in cancer. *Nature* 411: 342–348.
- DeBerardinis, R. J., J. J. Lum, G. Hatzivassiliou, and C. B. Thompson. 2008. The biology of cancer: metabolic reprogramming fuels cell growth and proliferation. *Cell Metab.* 7: 11–20.
- Perk, J., A. Iavarone, and R. Benezra. 2005. Id family of helix-loop-helix proteins in cancer. *Nat. Rev. Cancer* 5: 603–614.
- Lasorella, A., R. Benezra, and A. Iavarone. 2014. The ID proteins: master regulators of cancer stem cells and tumour aggressiveness. *Nat. Rev. Cancer* 14: 77–91.
- Hasskarl, J., and K. Münger. 2002. Id proteins—tumor markers or oncogenes? *Cancer Biol. Ther.* 1: 91–96.
- Shepherd, T. G., B. L. Thériault, and M. W. Nachtigal. 2008. Autocrine BMP4 signalling regulates ID3 proto-oncogene expression in human ovarian cancer cells. *Gene* 414: 95–105.
- Lee, S. H., E. Hao, A. Kiselyuk, J. Shapiro, D. J. Shields, A. Lowy, F. Levine, and P. Itkin-Ansari. 2011. The ID3/E47 axis mediates cell-cycle control in human pancreatic ducts and adenocarcinoma. *Mol. Cancer Res.* 9: 782–790.
- O'Brien, C. A., A. Kreso, P. Ryan, K. G. Hermans, L. Gibson, Y. Wang, A. Tsatsanis, S. Gallinger, and J. E. Dick. 2012. ID1 and ID3 regulate the self-renewal capacity of human colon cancer-initiating cells through p21. *Cancer Cell* 21: 777–792.
- DiVito, K. A., C. M. Simbulan-Rosenthal, Y. S. Chen, V. A. Trabosh, and D. S. Rosenthal. 2014. Id2, Id3 and Id4 overcome a Smad7-mediated block in tumorigenesis, generating TGF- β -independent melanoma. *Carcinogenesis* 35: 951–958.
- Tsuchiya, T., Y. Okaji, N. H. Tsuno, D. Sakurai, N. Tsuchiya, K. Kawai, K. Yazawa, M. Asakage, J. Yamada, S. Yoneyama, et al. 2005. Targeting Id1 and Id3 inhibits peritoneal metastasis of gastric cancer. *Cancer Sci.* 96: 784–790.
- Sharma, P., D. Patel, and J. Chaudhary. 2012. Id1 and Id3 expression is associated with increasing grade of prostate cancer: Id3 preferentially regulates CDKN1B. *Cancer Med.* 1: 187–197.
- Kamalian, L., S. S. Forootan, Z. Z. Bao, Y. Zhang, J. R. Gosney, C. S. Foster, and Y. Ke. 2010. Inhibition of tumorigenicity of small cell lung cancer cells by suppressing Id3 expression. *Int. J. Oncol.* 37: 595–603.
- Gray, M. J., N. A. Dallas, G. Van Buren, L. Xia, A. D. Yang, R. J. Somcio, P. Gaur, L. S. Mangala, P. E. Vivas-Mejia, F. Fan, et al. 2008. Therapeutic targeting of Id2 reduces growth of human colorectal carcinoma in the murine liver. *Oncogene* 27: 7192–7200.
- Love, C., Z. Sun, D. Jima, G. Li, J. Zhang, R. Miles, K. L. Richards, C. H. Dunphy, W. W. Choi, G. Srivastava, et al. 2012. The genetic landscape of mutations in Burkitt lymphoma. *Nat. Genet.* 44: 1321–1325.
- Richter, J., M. Schlesner, S. Hoffmann, M. Kreuz, E. Leich, B. Burkhardt, M. Rosolowski, O. Ammerpohl, R. Wagener, S. H. Bernhart, et al. ICGC MML-Seq Project. 2012. Recurrent mutation of the ID3 gene in Burkitt lymphoma identified by integrated genome, exome and transcriptome sequencing. *Nat. Genet.* 44: 1316–1320.
- Schmitz, R., M. Ceribelli, S. Pittaluga, G. Wright, and L. M. Staudt. 2014. Oncogenic mechanisms in Burkitt lymphoma. *Cold Spring Harb. Perspect. Med.* 4:a014282.
- Li, J., T. Maruyama, P. Zhang, J. E. Konkel, V. Hoffman, B. Zamarron, and W. Chen. 2010. Mutation of inhibitory helix-loop-helix protein Id3 causes $\gamma\delta$ T-cell lymphoma in mice. *Blood* 116: 5615–5621.
- Yu, L., C. Liu, J. Vandeusen, B. Becknell, Z. Dai, Y. Z. Wu, A. Ravai, T. H. Liu, W. Ding, C. Mao, et al. 2005. Global assessment of promoter methylation in a mouse model of cancer identifies ID4 as a putative tumor-suppressor gene in human leukemia. *Nat. Genet.* 37: 265–274.
- Chen, S. S., R. Claus, D. M. Lucas, L. Yu, J. Qian, A. S. Ruppert, D. A. West, K. E. Williams, A. J. Johnson, F. Sablitzky, et al. 2011. Silencing of the inhibitor of DNA binding protein 4 (ID4) contributes to the pathogenesis of mouse and human CLL. *Blood* 117: 862–871.
- Ren, Y., H. W. Cheung, G. von Maltzhan, A. Agrawal, G. S. Cowley, B. A. Weir, J. S. Boehm, P. Tamayo, A. M. Karst, J. F. Liu, et al. 2012. Targeted tumor-penetrating siRNA nanocomplexes for credentialing the ovarian cancer oncogene ID4. *Sci. Transl. Med.* 4: 147ra112.
- Russell, R. G., A. Lasorella, L. E. Dettin, and A. Iavarone. 2004. Id2 drives differentiation and suppresses tumor formation in the intestinal epithelium. *Cancer Res.* 64: 7220–7225.
- Benezra, R., R. L. Davis, D. Lockshon, D. L. Turner, and H. Weintraub. 1990. The protein Id: a negative regulator of helix-loop-helix DNA binding proteins. *Cell* 61: 49–59.
- Engel, I., and C. Murre. 2001. The function of E- and Id proteins in lymphocyte development. *Nat. Rev. Immunol.* 1: 193–199.
- Kee, B. L. 2009. E and ID proteins branch out. *Nat. Rev. Immunol.* 9: 175–184.
- Ueda-Hayakawa, I., J. Mahlios, and Y. Zhuang. 2009. Id3 restricts the developmental potential of gamma delta lineage during thymopoiesis. *J. Immunol.* 182: 5306–5316.
- Alonzo, E. S., and D. B. Sant'Angelo. 2011. Development of PLZF-expressing innate T cells. *Curr. Opin. Immunol.* 23: 220–227.
- Alonzo, E. S., R. A. Gottschalk, J. Das, T. Egawa, R. M. Hobbs, P. P. Pandolfi, P. Pereira, K. E. Nichols, G. A. Koretzky, M. S. Jordan, and D. B. Sant'Angelo. 2010. Development of promyelocytic zinc finger and ThPOK-expressing innate gamma delta T cells is controlled by strength of TCR signaling and Id3. *J. Immunol.* 184: 1268–1279.
- Verykokakis, M., M. D. Boos, A. Bendelac, E. J. Adams, P. Pereira, and B. L. Kee. 2010. Inhibitor of DNA binding 3 limits development of murine slam-associated adaptor protein-dependent “innate” gammadelta T cells. *PLoS One* 5: e9303.
- Verykokakis, M., V. Krishnamoorthy, A. Iavarone, A. Lasorella, M. Sigvardsson, and B. L. Kee. 2013. Essential functions for ID proteins at multiple checkpoints in invariant NKT cell development. *J. Immunol.* 191: 5973–5983.
- Zhang, B., Y. Y. Lin, M. Dai, and Y. Zhuang. 2014. Id3 and Id2 act as a dual safety mechanism in regulating the development and population size of innate-like $\gamma\delta$ T cells. *J. Immunol.* 192: 1055–1063.

34. Li, J., D. Wu, N. Jiang, and Y. Zhuang. 2013. Combined deletion of Id2 and Id3 genes reveals multiple roles for E proteins in invariant NKT cell development and expansion. *J. Immunol.* 191: 5052–5064.
35. Roy, S., and Y. Zhuang. 2015. Orchestration of invariant natural killer T cell development by E and Id proteins. *Crit. Rev. Immunol.* 35: 33–48.
36. D'Cruz, L. M., M. H. Stradner, C. Y. Yang, and A. W. Goldrath. 2014. E and Id proteins influence invariant NKT cell sublineage differentiation and proliferation. *J. Immunol.* 192: 2227–2236.
37. Hu, T., H. Wang, A. Simmons, S. Bajiña, Y. Zhao, S. Kovats, X. H. Sun, and J. Alberola-Ila. 2013. Increased level of E protein activity during invariant NKT development promotes differentiation of invariant NKT2 and invariant NKT17 subsets. *J. Immunol.* 191: 5065–5073.
38. Bendelac, A., M. Bonneville, and J. F. Kearney. 2001. Autoreactivity by design: innate B and T lymphocytes. *Nat. Rev. Immunol.* 1: 177–186.
39. Dranoff, G. 2004. Cytokines in cancer pathogenesis and cancer therapy. *Nat. Rev. Cancer* 4: 11–22.
40. Vivier, E., S. Ugolini, D. Blaise, C. Chabannon, and L. Brossay. 2012. Targeting natural killer cells and natural killer T cells in cancer. *Nat. Rev. Immunol.* 12: 239–252.
41. Godfrey, D. I., and M. Kronenberg. 2004. Going both ways: immune regulation via CD1d-dependent NKT cells. *J. Clin. Invest.* 114: 1379–1388.
42. Margulies, D. H. 2014. The in-betweeners: MAIT cells join the innate-like lymphocytes gang. *J. Exp. Med.* 211: 1501–1502.
43. Bendelac, A., P. B. Savage, and L. Teyton. 2007. The biology of NKT cells. *Annu. Rev. Immunol.* 25: 297–336.
44. Matsuo, Y., and H. G. Drexler. 2003. Immunoprofiling of cell lines derived from natural killer-cell and natural killer-like T-cell leukemia-lymphoma. *Leuk. Res.* 27: 935–945.
45. Ritchie, M. E., B. Phipson, D. Wu, Y. Hu, C. W. Law, W. Shi, and G. K. Smyth. 2015. Limma powers differential expression analyses for RNA-sequencing and microarray studies. *Nucleic Acids Res.* 43: e47.
46. Heng, T. S., M. W. Painter, Immunological Genome Project Consortium. 2008. The Immunological Genome Project: networks of gene expression in immune cells. *Nat. Immunol.* 9: 1091–1094.
47. Glaab, E., J. M. Garibaldi, and N. Krasnogor. 2009. ArrayMining: a modular web-application for microarray analysis combining ensemble and consensus methods with cross-study normalization. *BMC Bioinformatics* 10: 358.
48. Micallef, L., and P. Rodgers. 2014. eulerAPE: drawing area-proportional 3-Venn diagrams using ellipses. *PLoS ONE* 9: e101717.
49. Heinz, S., C. Benner, N. Spann, E. Bertolino, Y. C. Lin, P. Laslo, J. X. Cheng, C. Murte, H. Singh, and C. K. Glass. 2010. Simple combinations of lineage-determining transcription factors prime cis-regulatory elements required for macrophage and B cell identities. *Mol. Cell* 38: 576–589.
50. Miyazaki, M., K. Miyazaki, S. Chen, V. Chandra, K. Wagatsuma, Y. Agata, H. R. Rodewald, R. Saito, A. N. Chang, N. Varki, et al. 2015. The E-Id protein axis modulates the activities of the PI3K-AKT-mTORC1-Hif1a and c-myc/p19Arf pathways to suppress innate variant TFH cell development, thymocyte expansion, and lymphomagenesis. *Genes Dev.* 29: 409–425.
51. Kovalovsky, D., O. U. Uche, S. Eladad, R. M. Hobbs, W. Yi, E. Alonzo, K. Chua, M. Eidson, H. J. Kim, J. S. Im, et al. 2008. The BTB-zinc finger transcriptional regulator PLZF controls the development of invariant natural killer T cell effector functions. *Nat. Immunol.* 9: 1055–1064.
52. Vervakakis, M., M. D. Boos, A. Bendelac, and B. L. Kee. 2010. SAP protein-dependent natural killer T-like cells regulate the development of CD8(+) T cells with innate lymphocyte characteristics. *Immunity* 33: 203–215.
53. Miyazaki, M., R. R. Rivera, K. Miyazaki, Y. C. Lin, Y. Agata, and C. Murte. 2011. The opposing roles of the transcription factor E2A and its antagonist Id3 that orchestrate and enforce the naive fate of T cells. *Nat. Immunol.* 12: 992–1001.
54. Godfrey, D. I., H. R. MacDonald, M. Kronenberg, M. J. Smyth, and L. Van Kaer. 2004. NKT cells: what's in a name? *Nat. Rev. Immunol.* 4: 231–237.
55. El-Guendy, N., and V. M. Rangnekar. 2003. Apoptosis by Par-4 in cancer and neurodegenerative diseases. *Exp. Cell Res.* 283: 51–66.
56. Perillo, N. L., K. E. Pace, J. J. Seilhamer, and L. G. Baum. 1995. Apoptosis of T cells mediated by galectin-1. *Nature* 378: 736–739.
57. Marigo, I., E. Bosio, S. Solito, C. Mesa, A. Fernandez, L. Dolcetti, S. Ugel, N. Sonda, S. Bicchato, E. Falisi, et al. 2010. Tumor-induced tolerance and immune suppression depend on the C/EBPbeta transcription factor. *Immunity* 32: 790–802.
58. Yanai, H., H. M. Chen, T. Inuzuka, S. Kondo, T. W. Mak, A. Takaoka, K. Honda, and T. Taniguchi. 2007. Role of IFN regulatory factor 5 transcription factor in antiviral immunity and tumor suppression. *Proc. Natl. Acad. Sci. USA* 104: 3402–3407.
59. Shen, S., J. Wu, S. Srivatsan, B. K. Gorentla, J. Shin, L. Xu, and X. P. Zhong. 2011. Tight regulation of diacylglycerol-mediated signaling is critical for proper invariant NKT cell development. *J. Immunol.* 187: 2122–2129.
60. Dominguez, C. L., D. H. Floyd, A. Xiao, G. R. Mullins, B. A. Kefas, W. Xin, M. N. Yacur, R. Abounader, J. K. Lee, G. M. Wilson, et al. 2013. Diacylglycerol kinase α is a critical signaling node and novel therapeutic target in glioblastoma and other cancers. *Cancer Discov.* 3: 782–797.
61. Ohki, R., J. Nemoto, H. Murasawa, E. Oda, J. Inazawa, N. Tanaka, and T. Taniguchi. 2000. Reprimo, a new candidate mediator of the p53-mediated cell cycle arrest at the G2 phase. *J. Biol. Chem.* 275: 22627–22630.
62. Liu, X., N. Yang, S. A. Figel, K. E. Wilson, C. D. Morrison, I. H. Gelman, and J. Zhang. 2013. PTPN14 interacts with and negatively regulates the oncogenic function of YAP. *Oncogene* 32: 1266–1273.
63. Winkler, G. S. 2010. The mammalian anti-proliferative BTG/Tob protein family. *J. Cell. Physiol.* 222: 66–72.
64. Zou, Z., F. Zeng, W. Xu, C. Wang, Z. Ke, Q. J. Wang, and F. Deng. 2012. PKD2 and PKD3 promote prostate cancer cell invasion by modulating NF- κ B- and HDAC1-mediated expression and activation of uPA. *J. Cell Sci.* 125: 4800–4811.
65. Pellikainen, J. M., K. M. Ropponen, V. V. Kataja, J. K. Kellokoski, M. J. Eskelinen, and V. M. Kosma. 2004. Expression of matrix metalloproteinase (MMP)-2 and MMP-9 in breast cancer with a special reference to activator protein-2, HER2, and prognosis. *Clin. Cancer Res.* 10: 7621–7628.
66. Oehler, M. K., C. Norbury, S. Hague, M. C. Rees, and R. Bicknell. 2001. Adrenomedullin inhibits hypoxic cell death by upregulation of Bcl-2 in endometrial cancer cells: a possible promotion mechanism for tumour growth. *Oncogene* 20: 2937–2945.
67. Banks, R. E., A. J. Gearing, I. K. Hemingway, D. R. Norfolk, T. J. Perren, and P. J. Selby. 1993. Circulating intercellular adhesion molecule-1 (ICAM-1), E-selectin and vascular cell adhesion molecule-1 (VCAM-1) in human malignancies. *Br. J. Cancer* 68: 122–124.
68. Johnston, B., C. H. Kim, D. Soler, M. Emoto, and E. C. Butcher. 2003. Differential chemokine responses and homing patterns of murine TCR alpha beta NKT cell subsets. *J. Immunol.* 171: 2960–2969.
69. D'Cruz, L. M., J. Knell, J. K. Fujimoto, and A. W. Goldrath. 2010. An essential role for the transcription factor HEB in thymocyte survival, Tcr rearrangement and the development of natural killer T cells. *Nat. Immunol.* 11: 240–249.
70. Elewaut, D., R. B. Shaikh, K. J. Hammond, H. De Winter, A. J. Leishman, S. Sidobre, O. Turovskaya, T. I. Prigozy, L. Ma, T. A. Banks, et al. 2003. NIK-dependent RelB activation defines a unique signaling pathway for the development of V alpha 14i NKT cells. *J. Exp. Med.* 197: 1623–1633.
71. Fukasawa, K. 2005. Centrosome amplification, chromosome instability and cancer development. *Cancer Lett.* 230: 6–19.
72. Lamprecht B., Walter K., Kreher S., Kumar R., Hummel M., Lenze D., Kochert K., Bouhrel M. A., Richter J., Soler E., et al. 2010. Derepression of an endogenous long terminal repeat activates the CSF1R proto-oncogene in human lymphoma. *Nat. Med.* 16: 571–579, 1p following 579.
73. Koizumi, K., S. Hojo, T. Akashi, K. Yasumoto, and I. Saiki. 2007. Chemokine receptors in cancer metastasis and cancer cell-derived chemokines in host immune response. *Cancer Sci.* 98: 1652–1658.
74. Zlotnik, A., A. M. Burkhardt, and B. Homey. 2011. Homeostatic chemokine receptors and organ-specific metastasis. *Nat. Rev. Immunol.* 11: 597–606.
75. Franitza, S., V. Grabovsky, O. Wald, I. Weiss, K. Beider, M. Dagan, M. Darash-Yahana, A. Nagler, S. Brocke, E. Galun, et al. 2004. Differential usage of VLA-4 and CXCR4 by CD3+CD56+ NKT cells and CD56+CD16+ NK cells regulates their interaction with endothelial cells. *Eur. J. Immunol.* 34: 1333–1341.
76. Emoto, M., H. W. Mittrücker, R. Schmits, T. W. Mak, and S. H. Kaufmann. 1999. Critical role of leukocyte function-associated antigen-1 in liver accumulation of CD4+NKT cells. *J. Immunol.* 162: 5094–5098.
77. Teicher, B. A., and S. P. Fricker. 2010. CXCL12 (SDF-1)/CXCR4 pathway in cancer. *Clin. Cancer Res.* 16: 2927–2931.
78. Imai, H., N. Sunaga, Y. Shimizu, S. Kakegawa, K. Shimizu, T. Sano, T. Ishizuka, T. Oyama, R. Saito, J. D. Minna, and M. Mori. 2010. Clinicopathological and therapeutic significance of CXCL12 expression in lung cancer. *Int. J. Immunopathol. Pharmacol.* 23: 153–164.
79. Franki, A. S., K. Van Beneden, P. Dewint, K. J. Hammond, S. Lambrecht, G. Leclercq, M. Kronenberg, D. Deforce, and D. Elewaut. 2006. A unique lymphotoxin alphabeta-dependent pathway regulates thymic emigration of Valpha14 invariant natural killer T cells. *Proc. Natl. Acad. Sci. USA* 103: 9160–9165.
80. Blyth, K., F. Vaillant, L. Hanlon, N. Mackay, M. Bell, A. Jenkins, J. C. Neil, and E. R. Cameron. 2006. Runx2 and MYC collaborate in lymphoma development by suppressing apoptotic and growth arrest pathways in vivo. *Cancer Res.* 66: 2195–2201.
81. Egeblad, M., and Z. Werb. 2002. New functions for the matrix metalloproteinases in cancer progression. *Nat. Rev. Cancer* 2: 161–174.
82. Sternlicht, M. D., A. Lochter, C. J. Sympon, B. Huey, J. P. Rougier, J. W. Gray, D. Pinkel, M. J. Bissell, and Z. Werb. 1999. The stromal proteinase MMP3/stromelysin-1 promotes mammary carcinogenesis. *Cell* 98: 137–146.
83. Bouchard, F., S. D. Bélanger, K. Biron-Pain, and Y. St-Pierre. 2010. EGR-1 activation by EGF inhibits MMP-9 expression and lymphoma growth. *Blood* 116: 759–766.
84. Niola, F., X. Zhao, D. Singh, A. Castano, R. Sullivan, M. Lauria, H. S. Nam, Y. Zhuang, R. Benezra, D. Di Bernardo, et al. 2012. Id proteins synchronize stemness and anchorage to the niche of neural stem cells. *Nat. Cell Biol.* 14: 477–487.
85. Starlets, D., Y. Gore, I. Binsky, M. Haran, N. Harpaz, L. Shvidel, S. Becker-Herman, A. Berrebi, and I. Shachar. 2006. Cell-surface CD74 initiates a signaling cascade leading to cell proliferation and survival. *Blood* 107: 4807–4816.
86. Wang, W., T. Yuasa, N. Tsuchiya, Z. Ma, S. Maita, S. Narita, T. Kumazawa, T. Inoue, H. Tsuruta, Y. Horikawa, et al. 2009. The novel tumor-suppressor Mel-18 in prostate cancer: its functional polymorphism, expression and clinical significance. *Int. J. Cancer* 125: 2836–2843.
87. Cowan, J. E., N. I. McCarthy, S. M. Parnell, A. J. White, A. Bacon, A. Serge, M. Irla, P. J. Lane, E. J. Jenkinson, W. E. Jenkinson, and G. Anderson. 2014. Differential requirement for CCR4 and CCR7 during the development of innate and adaptive α BT cells in the adult thymus. *J. Immunol.* 193: 1204–1212.
88. Lazarevic, V., A. J. Zullo, M. N. Schweitzer, T. L. Staton, E. M. Gallo, G. R. Crabtree, and L. H. Glimcher. 2009. The gene encoding early growth response 2, a target of the transcription factor NFAT, is required for the development and maturation of natural killer T cells. *Nat. Immunol.* 10: 306–313.

89. Seiler, M. P., R. Mathew, M. K. Liszewski, C. J. Spooner, K. Barr, F. Meng, H. Singh, and A. Bendelac. 2012. Elevated and sustained expression of the transcription factors *Egr1* and *Egr2* controls NKT lineage differentiation in response to TCR signaling. [Published erratum appears in 2013 *Nat. Immunol.* 14: 413.] *Nat. Immunol.* 13: 264–271.
90. Jiang, L., Z. H. Gu, Z. X. Yan, X. Zhao, Y. Y. Xie, Z. G. Zhang, C. M. Pan, Y. Hu, C. P. Cai, Y. Dong, et al. 2015. Exome sequencing identifies somatic mutations of *DDX3X* in natural killer/T-cell lymphoma. *Nat. Genet.* 47: 1061–1066.
91. Bachy, E., M. Urb, S. Chandra, R. Robinot, G. Bricard, S. de Bernard, A. Traverse-Glehen, S. Gazzo, O. Blond, A. Khurana, et al. 2016. CD1d-restricted peripheral T cell lymphoma in mice and humans. *J. Exp. Med.* 213: 841–857.
92. Belle, I., J. Mahlios, A. McKenzie, and Y. Zhuang. 2014. Aberrant production of IL-13 by T cells promotes exocrinopathy in Id3 knockout mice. *Cytokine* 69: 226–233.
93. Prince, A. L., L. B. Watkin, C. C. Yin, L. K. Selin, J. Kang, P. L. Schwartzberg, and L. J. Berg. 2014. Innate PLZF+CD4+ $\alpha\beta$ T cells develop and expand in the absence of *Itk*. *J. Immunol.* 193: 673–687.
94. Yu, J., T. Mitsui, M. Wei, H. Mao, J. P. Butchar, M. V. Shah, J. Zhang, A. Mishra, C. Alvarez-Breckenridge, X. Liu, et al. 2011. NKp46 identifies an NKT cell subset susceptible to leukemic transformation in mouse and human. *J. Clin. Invest.* 121: 1456–1470.
95. McGregor, S., A. Shah, G. Raca, M. K. Mirza, S. M. Smith, J. Anastasi, J. W. Vardiman, E. Hyjek, and S. Gurbuxani. 2014. PLZF staining identifies peripheral T-cell lymphomas derived from innate-like T-cells with TRAV1-2-TRAJ33 TCR- α rearrangement. *Blood* 123: 2742–2743.
96. Ogata, H., S. Goto, K. Sato, W. Fujibuchi, H. Bono, and M. Kanehisa. 1999. KEGG: Kyoto Encyclopedia of Genes and Genomes. *Nucleic Acids Res.* 27: 29–34